Supplementary Information for: "Pulsed excitation dynamics of a nanoscale optomechanical resonator near its quantum ground-state of motion"

Seán M. Meenehan,[1,2] Justin D. Cohen,[1,2] Gregory S. MacCabe,[1,2]
Francesco Marsili,[3] Matthew D. Shaw,[3] and Oskar Painter[1,2,*]

[1]*Kavli Nanoscience Institute and Thomas J. Watson, Sr., Laboratory of Applied Physics, California Institute of Technology, Pasadena, CA 91125, USA*
[2]*Institute for Quantum Information and Matter, California Institute of Technology, Pasadena, CA 91125, USA*
[3]*Jet Propulsion Laboratory, California Institute of Technology, Pasadena, CA 91109, USA*
(Dated: July 6, 2015)

FABRICATION

The devices are fabricated from a silicon-on-insulator (SOI) wafer (SOITEC, 220 nm device layer, 3 μm buried oxide) using electron beam lithography followed by reactive ion etching (RIE/ICP). The Si device layer is then masked using ProTEK PSB photoresist to define a mesa region of the chip to which a tapered lensed fiber can access. Outside of the protected mesa region, the buried oxide is removed with a plasma etch and a trench is formed in the underlying silicon substrate using tetramethylammonium hydroxide (TMAH). The devices are then released in hydrofluoric acid (49 % aqueous HF solution) and cleaned in a piranha solution (3-to-1 H_2SO_4:H_2O_2) before a final hydrogen termination in diluted HF. In fabrication, arrays of the nominal design are scaled by ± 2 % to account for frequency shifts due to fabrication imperfections and disorder.

EXPERIMENTAL SETUP

The full measurement setup is shown in Fig. S-1. A fiber-coupled, wavelength tunable external cavity diode laser is used as the light source, with a small portion ($\sim 1\%$) of the laser output sent to a wavemeter (λ-meter) for frequency stabilization. The remaining laser power is sent through both a C-band optical demultiplexer (DeMux) to reject broadband spontaneous emission from the laser, and a high-finesse tunable filter to remove laser phase noise at the mechanical frequency, which can both contribute to excess pump transmission noise on the single photon detector [1]. After pre-filtering, the laser pump is sent through an electro-optic phase modulator (ϕ-m) which may be driven by either an RF signal generator, to generate optical sidebands for locking the filter cavities, or a vector network analyzer (VNA) for obtaining the amplitude and phase response of the optical cavity.

To generate pulses, an optical switch (SW1) allows the pump tone to be sent through a series of electro-optic amplitude modulators for the generation of optical pulses. The first is a fast high-extinction modulator (a-m) with a rise and fall time of ~ 25 ns. Though in principle the high-extinction modulator can provide $50-60$ dB extinction on its own, its transmission level is much less stable and difficult to lock at the maximum extinction point. Thus, we lock the modulator at ~ 30 dB of extinction and use two electro-optic switches, each providing $\sim 18-20$ dB extinction, to fully extinguish the pump. While these switches are much slower (~ 200 ns rise time, ~ 30 μs fall time), the extra switching time should have a negligible impact as it is much smaller than the pulse periods used here (~ 1 ms or more). The modulators are collectively driven by a variable delay electrical pulse generator which also provides a synchronization pulse to the single photon counting electronics.

A variable optical attenuator (VOA) controls the power input to the cavity, after which an optical circulator routes the laser light to a lensed fiber tip inside the dilution refrigerator for end-fire coupling to the device. Subsequently, the cavity reflection can be switched (SW3) into one of two detection setups. The first setup sends the signal through an erbium-doped fiber amplifier (EDFA) followed by a high-speed photodetector (PD). The resulting amplified photocurrent may be directed to a real-time spectrum analyzer (RSA) in order to measure the optical noise power spectral density (NPSD) for mechanical characterization or to the VNA which is used in conjunction with the phase modulator to measure the full complex response of the optical cavity for purposes of optical characterization as described below. The second detection path sends the reflected signal through three additional tunable filters in order to reject the pump frequency, and then back into the dilution refrigerator where it is detected by a superconducting single photon detector (SPD). The output of this detector is sent to a time-correlated single photon counting (TCSPC) module to build up a histogram of photon count events as a function of time relative to the synchronization pulse received from the pulse generator.

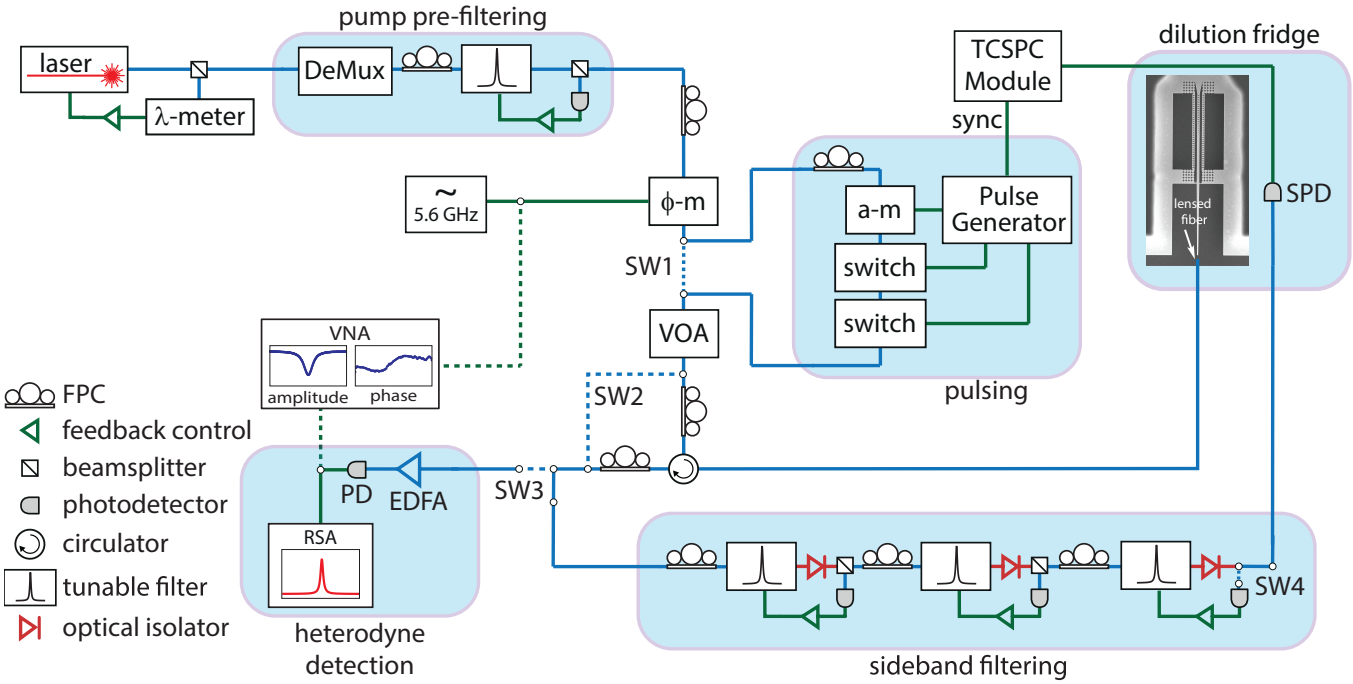

FIG. S-1: **Experimental setup.** Full setup for performing pulsed phonon counting. λ-meter: wavemeter, DeMux: C-band optical demultiplexer, ϕ-m: electro-optic phase modulator, SW: optical switch, a-m: high-extinction electro-optic amplitude modulator, switch: high-speed electro-optic switch, VOA: variable optical attenuator, EDFA: erbium-doped fiber amplifier, PD: high-speed photodetector, RSA: real-time spectrum analyzer, VNA: vector network analyzer, SPD: single photon detector, TCSPC: time-correlated single photon counting, FPC: fiber polarization controller..

The SPDs used in this work are amorphous WSi-based superconducting nanowire single-photon detectors developed in collaboration between the Jet Propulsion Laboratory and NIST. The SPDs are design for high-efficiency detection of individual photons in the wavelength range $\lambda = 1520 - 1610$ nm with maximum count rates as large as 10^7 counts per second (c.p.s) [2]. The SPDs are mounted on the still stage of the dilution refrigerator at ~ 700 mK. Single-mode optical fibers (Corning SMF-28) are passed into the refrigerator through vacuum feedthroughs and coupled to the SPDs via a fiber sleeve attached to each SPD mount. Proper alignment of the incoming fiber with the 15 μm $\times$ 15 μm square area of the SPD nanowire is ensured by a self-aligned mounting system incorporated into the design of the SPD [2]. The radio-frequency output of each SPD is amplified by a cold-amplifier mounted on the 50 K stage of the refrigerator as well as a room-temperature amplifier, then read out by a triggered PicoQuant PicoHarp 300 time-correlated single photon counting module. By systematically isolating the input optical fiber from environmental light sources and filtering out long wavelength blackbody radiation inside the fridge we have achieved dark count rates of ~ 4 (c.p.s.). At just below the switching current of the detectors, we have measured a peak detection efficiency of $\eta_{\mathrm{SPD}} = 68\%$, with $\lesssim 20\%$ variability depending on photon polarization.

The tunable filters used for both pre-filtering the pump and filtering the cavity reflection are commercially available, piezo-tunable Fabry-Perot filters (Micron Optics, FFP-TF2), all with a ~ 50 MHz bandwidth, a free-spectral range of ~ 20 GHz, and a tuning voltage of $\lesssim 18$ V per free-spectral range. The filters each offer roughly 40 dB of pump suppression (relative to the peak transmission) measured at a filter-pump varies by $1-2$ dB from filter to filter. When locking the post-cavity filters a switch is used to bypass the cavity (SW2), as a relatively large amount of CW power is used during the locking procedure and we would like to avoid sending large amounts of power into the cavity unless necessary. More importantly, the SPD is also bypassed (SW4), as allowing too much power to reach the SPD will saturate it resulting in significantly elevated dark counts ($\Gamma_{\mathrm{dark}} \approx 500 - 1000$ c.p.s.) for $1-2$ minutes after the signal is turned off. Once the switches are set an RF signal generator is used to drive the phase modulator at ω_{m}, producing an optical sideband which is aligned with the cavity (and motional sideband) frequency. To lock the filter chain, a sinusoidal voltage (with an initial range of ± 10 V) is used to dither each filter while monitoring its transmission. The offsets of the sinusoids are then adjusted, and their amplitudes reduced, to maximize transmission of the desired sideband, fixing the voltages once all three filters are well aligned. Over time the filters will drift and the locking

procedure will need to be repeated, though in subsequent re-locking attempts a much smaller dithering amplitude of ~ 1 V is sufficient. As the piezo elements controlling each filter have a finite settling time, the filters will drift much more rapidly following the initial locking attempt (during which large voltage shifts are applied) than following subsequent re-locks. After several re-locks, the filters will typically become stable enough that the total transmission at the sideband frequency changes by $\lesssim 5\%$ over several minutes. At this point the phase modulator is turned off, the pulse generator, cavity and SPD are switched back into the optical train and we begin accumulating pulsed data for 2 minutes before re-locking the filters. The total filter transmission is recorded at the end of a locking procedure and again prior to re-locking, and if the transmission has shifted by more than a few percent the previous pulsed dataset is discarded. All the time-resolved data shown in this chapter are taken in this manner, with all 2 minutes datasets averaged together to produce the final pulsed histogram.

DEVICE CHARACTERIZATION

The measurements presented in this work rely on an accurate calibration of the optomechanical damping rate γ_{OM}, which depends on the vacuum optomechanical coupling rate g_0, the total optical decay rate κ, and the intracavity photon number n_{c}. The photon number for a given power and detuning in turn depends on the single pass fiber-to-waveguide coupling efficiency η_{cpl} and waveguide-cavity coupling efficiency $\eta_\kappa = \kappa_{\mathrm{e}}/\kappa$ (κ_{e} is the waveguide-cavity coupling rate). The fiber collection efficiency is determined by measuring the calibrated reflection level far-off resonance with the optical cavity on the optical power meter, and is found to be $\eta_{\mathrm{cpl}} = 0.68$ for the device measured here (total device reflection efficiency of $\sim 0.46\%$). To measure κ and η_κ, the laser is placed off-resonance from the cavity and the VNA is used to drive the phase modulator and sweep an optical sideband across the cavity. By detecting the reflection on a high-speed photodiode connected to the VNA input we obtain the amplitude and phase response of the cavity from which can extract $\kappa/2\pi = 443$ MHz (corresponding to an optical quality factor of $Q_{\mathrm{o}} \approx 4.4 \times 10^5$), and $\eta_\kappa = 0.5$. With these three parameters measured, it is possible to determine n_{c} for an arbitrary input power to the cavity.

To characterize the acoustic resonance, the EDFA is used to amplify the cavity reflection so that the optical noise floor overcomes the photodetector's electronic noise and the optical NPSD is measured on the RSA, where a Lorentzian response due to transduction of the acoustic thermal Brownian motion can be observed at the acoustic resonance frequency $\omega_{\mathrm{m}}/2\pi = 5.6$ GHz. For a red- or blue detuned pump laser ($\Delta \equiv \omega_{\mathrm{c}} - \omega_{\mathrm{l}} = \pm\omega_{\mathrm{m}}$) the linewidth of this transduced noise peak is $\gamma = \gamma_{\mathrm{b}} \pm \gamma_{\mathrm{OM}}$, where γ_{b} is the bare coupling rate of the mechanical resonator to its bath and $\gamma_{\mathrm{OM}} \equiv 4g_0^2 n_{\mathrm{c}}/\kappa$. Thus, by averaging the observed linewidth for red- and blue-detuned pumps we can determine γ_{b} and thus extract the excess optomechanically induced damping rate γ_{OM} as a function of n_{c}. With n_{c} and κ determined, a linear fit of γ_{OM} reveals a vacuum optomechanical coupling rate of $g_0/2\pi = 710$ kHz.

PHONON COUNTING

In the linearized sideband resolved regime with a red-detuned pump ($\Delta = \omega_{\mathrm{m}}$) the total reflected cavity amplitude will be sum of the coherent pump reflection α_{out} and a fluctuation term given, in the Fourier domain and in a frame rotating at the pump frequency, by [3]

$$\hat{a}_{\mathrm{out}}(\omega)|_{\Delta=\omega_{\mathrm{m}}} \approx r(\omega)\hat{a}_{\mathrm{in}}(\omega) + n(\omega)\hat{a}_{\mathrm{i}}(\omega) + s(\omega)\hat{b}_{\mathrm{in}}(\omega), \tag{S-1}$$

where $\hat{a}_{\mathrm{in}}$ and $\hat{a}_{\mathrm{i}}$ are the pump noise and intrinsic cavity noise, respectively (assumed for the moment to be vacuum noise), $\hat{b}_{\mathrm{in}}$ is the noise operator for the mechanical bath, which has the correlation function $\left\langle \hat{b}_{\mathrm{in}}^\dagger(\omega)\hat{b}^\dagger(\omega')\right\rangle = n_{\mathrm{b}}\delta(\omega + \omega')$ (n_{b} is the bath occupancy), and the effective scattering matrix elements are given by

$$r(\omega) = 1 - \frac{2\kappa_{\mathrm{e}}}{\kappa} \pm \frac{\gamma_{\mathrm{OM}}\kappa_{\mathrm{e}}}{\kappa}\frac{1}{\pm i\left(\omega_{\mathrm{m}} \mp \omega\right) + \gamma/2}, \tag{S-2}$$

$$n(\omega;\pm) = \pm\frac{\sqrt{\kappa_{\mathrm{i}}\kappa_{\mathrm{e}}}}{\kappa}\left(\frac{\gamma_{\mathrm{OM}}}{\pm i\left(\omega_{\mathrm{m}} \mp \omega\right) + \gamma/2} \mp 2\right), \tag{S-3}$$

$$s(\omega) = \sqrt{\frac{\kappa_{\mathrm{e}}}{\kappa}}\frac{i\sqrt{\gamma_{\mathrm{i}}\gamma_{\mathrm{OM}}}}{\pm i\left(\omega_{\mathrm{m}} \mp \omega\right) + \gamma/2}. \tag{S-4}$$

As the full reflected signal from the cavity includes the reflected pump amplitude, which is many orders of magnitude larger than the sideband signal, we must first filter the cavity output to reject the pump. Provided the filter is sufficiently high-finesse, it can be modeled in the frequency domain by a single Lorentzian function

$$F(\omega;\omega_{\mathrm{f}}) = \frac{\kappa_{\mathrm{f}}/2}{i(\omega_{\mathrm{f}}-\omega)+\kappa_{\mathrm{f}}/2}, \tag{S-5}$$

where κ_{f} and ω_{f} are the resonant frequency of the filter, respectively. Now, explicitly considering the case of red-detuned driving in the sideband-resolved regime, the filtered cavity output will be the product of $F(\omega;\omega_{\mathrm{f}})$ with the frequency domain output of the cavity. As the resonantly enhanced anti-Stokes sideband photons will be detuned by ω_{m} from the pump, we choose $\omega_{\mathrm{f}} = \omega_{\mathrm{m}}$. Using Eq. S-1, we obtain

$$\hat{a}_{\mathrm{filt}}(\omega) = F(\omega;\omega_{\mathrm{m}})\left(\alpha_{\mathrm{out}}\delta(\omega) + r(\omega;+)\hat{a}_{\mathrm{in}}(\omega) + n(\omega;+)\hat{a}_{\mathrm{i}}(\omega) + s(\omega;+)\hat{b}_{\mathrm{in}}(\omega)\right). \tag{S-6}$$

Performing photon counting on the filtered output then results in an average count rate of

$$\begin{aligned}
\Gamma(t) &= \left\langle \hat{a}^{\dagger}_{\mathrm{filt}}(t)\hat{a}_{\mathrm{filt}}(t)\right\rangle \\
&= \frac{1}{2\pi}\int_{-\infty}^{\infty} d\omega \int_{-\infty}^{\infty} d\omega'\; e^{i(\omega+\omega')t}\left\langle \hat{a}^{\dagger}_{\mathrm{filt}}(\omega)\hat{a}_{\mathrm{filt}}(\omega')\right\rangle \\
&= \frac{1}{2\pi}\left(|F(0;\omega_{\mathrm{m}})|^2|\alpha_{\mathrm{out}}|^2 + \frac{\kappa_{\mathrm{e}}}{\kappa}\gamma_{\mathrm{OM}}\int_{-\infty}^{\infty} d\omega |F(\omega;\omega_{\mathrm{m}})|^2\; S_{\mathrm{bb}}(\omega;\langle n\rangle)\right) \\
&\approx A|\alpha^2_{\mathrm{out}}| + \frac{\kappa_{\mathrm{e}}}{\kappa}\gamma_{\mathrm{OM}}\langle n\rangle,
\end{aligned} \tag{S-7}$$

where $A = \frac{1}{2\pi}|F(0;\omega_{\mathrm{m}})|^2$ is the pump attenuation factor, and $S_{\mathrm{bb}}(\omega;\langle n\rangle)$ is the phonon spectral density [3]

$$S_{\mathrm{bb}}(\omega) = \frac{\gamma\langle n\rangle}{(\omega_{\mathrm{m}}+\omega)^2 + (\gamma/2)^2}. \tag{S-8}$$

Note that we have assumed a filter bandwidth $\kappa_{\mathrm{f}} \gg \gamma$, allowing us to approximate $|F(\omega;\omega_{\mathrm{m}})|^2 \approx |F(\omega_{\mathrm{m}};\omega_{\mathrm{m}})|^2 = 1$ inside the integral over S_{bb}. A similar analysis for blue detuning (where $\omega_{\mathrm{f}} = -\omega_{\mathrm{m}}$ to filter the Stokes sideband) yields a comparable result, with $\langle n\rangle \to \langle n\rangle + 1$. Note that this formula assumes that $\hat{a}_{\mathrm{in}}$ and $\hat{a}_{\mathrm{i}}$ are vacuum noise, and thus do not contribute to counting of real photons.

The total count rate, including noise of the photon counter and reduction of the pump and signal due to measurement inefficiency, is given for red-detuning by

$$\Gamma_{\mathrm{tot}} = \Gamma_{\mathrm{dark}} + \Gamma_{\mathrm{pump}} + \eta\frac{\kappa_{\mathrm{e}}}{\kappa}\gamma_{\mathrm{OM}}\langle n\rangle, \tag{S-9}$$

where Γ_{dark} is the dark count rate of the photon detector, $\Gamma_{\mathrm{pump}} = \eta A|\alpha_{\mathrm{out}}|^2$ and η is the total measurement efficiency. These expressions can be used to perform thermometry in a similar fashion to linear detection, either by calibrating the cavity parameters and total measurement efficiency or by measuring the asymmetry between the red- and blue-detuned count rates.

To assess the sensitivity of this counting scheme, it is convenient to express the measurement noise floor $\Gamma_{\mathrm{dark}}+\Gamma_{\mathrm{pump}}$ in terms of an equivalent number of mechanical quanta (that is the mechanical occupancy $\langle n\rangle$ that would be needed to yield a signal-to-noise of one). This noise-equivalent phonon number is obtained by dividing the total noise floor by the per-phonon count rate $\Gamma_{\mathrm{SB},0} = \eta(\kappa_{\mathrm{e}}/\kappa)\gamma_{\mathrm{OM}}$, yielding

$$n_{\mathrm{NEP}} = \frac{\Gamma_{\mathrm{dark}} + \Gamma_{\mathrm{pump}}}{\Gamma_{\mathrm{SB},0}}. \tag{S-10}$$

For a highly sideband-resolved system, the reflected pump in the case of $\Delta = \pm\omega_{\mathrm{m}}$ will be approximately given by $\alpha_{\mathrm{out}} \approx \alpha_{\mathrm{in}}$. This in turn can be expressed in terms of the intracavity photon number as $|\alpha_{\mathrm{out}}|^2 \approx \omega_{\mathrm{m}}^2 n_{\mathrm{c}}/\kappa_{\mathrm{e}}$. Thus, n_{NEP} as a function of n_{c} is given by

$$n_{\mathrm{NEP}}(n_{\mathrm{c}}) = \frac{\kappa^2\Gamma_{\mathrm{dark}}}{4\eta\kappa_{\mathrm{e}}g_0^2 n_{\mathrm{c}}} + A\left(\frac{\kappa\omega_{\mathrm{m}}}{2\kappa_{\mathrm{e}}g_0}\right)^2. \tag{S-11}$$

EFFECTS OF TECHNICAL LASER NOISE

The mechanical frequency of the nanobeam used in this experiment ($\omega_\mathrm{m}/2\pi = 5.6$ GHz) raises concerns about the effects of laser phase noise on the measurements, as the laser used in this experiment has previously been observed to possess a prominent phase noise peak at 5 GHz [3]. In addition to phase noise, most diode lasers typically have a small amount of broadband spontaneous emission. While this additional noise is orders of magnitude weaker than the laser tone itself, it exists outside the wavelength region ($\lambda \sim 1520 - 1570$ nm) where the filters are guaranteed to be high finesse, and thus can be transmitted with high efficiency to the SPDs.

Phase noise in particular is worrisome as it can not only lead to an excess noise floor but also to real heating of the mechanics and systematic errors in thermometry due to noise squashing/anti-squashing [4, 5]. Phase noise can be accounted for by assuming a total pump noise operator given by [3]

$$\hat{a}_\mathrm{in,tot}(t) = \hat{a}_\mathrm{in}(t) + \hat{a}_\phi(t), \tag{S-12}$$

where $\hat{a}_\mathrm{in}(t)$ still represents vacuum noise and

$$\hat{a}_\phi(t) = i|\alpha_\mathrm{in}|\phi(t), \tag{S-13}$$

where $|\alpha_\mathrm{in}|$ is the amplitude of the pump and $\phi(t)$ is the stochastic phase of the pump, assumed to be a real, stationary Gaussian process with zero mean. The phase noise is assumed to be delta-correlated in the frequency domain, such that

$$\langle \phi(\omega)\phi(\omega')\rangle = S_{\phi\phi}(\omega)\delta(\omega+\omega'), \tag{S-14}$$

where the expectation value here corresponds to an ensemble average. The phase noise input to the cavity then has the correlation function

$$\left\langle \hat{a}_\phi^\dagger(\omega)\hat{a}_\phi(\omega')\right\rangle = S_{\alpha\alpha}(\omega)\delta(\omega+\omega'), \tag{S-15}$$

where $S_{\alpha\alpha}(\omega) = |\alpha|^2 S_{\phi\phi}(\omega)$. In a sideband-resolved system, for either red or blue detuning $\Delta = \pm\omega_\mathrm{m}$, we find that the presence of phase noise heats the mechanical resonator, with an additional added phonon occupancy given by [3]

$$\langle n\rangle_\phi|_{\Delta=\pm\omega_\mathrm{m}} = \frac{\kappa_\mathrm{e}}{\kappa}\frac{\gamma_\mathrm{OM}}{\gamma} n_\phi, \tag{S-16}$$

where we have defined $n_\phi = S_{\alpha\alpha}(\omega_\mathrm{m})$, and where we have assumed that $S_{\alpha\alpha}(\omega)$ is sufficiently slow-varying in the vicinity of $\omega = \omega_\mathrm{m}$ (specifically for $|\omega - \omega_\mathrm{m}| \lesssim \gamma$) that we may approximate $S_{\alpha\alpha}(\omega) = S_{\alpha\alpha}(\omega_\mathrm{m})$.

Including this additional noise term in the analysis of the previous section yields a phase noise contribution to the total photon count rate of

$$\Gamma_\phi|_{\Delta=\pm\omega_\mathrm{m}} = \eta\int_{-\infty}^{\infty}\frac{d\omega}{2\pi} S_{\alpha\alpha}(\omega)|F(\omega,\pm\omega_\mathrm{m})|^2|r(\omega;\pm)|^2. \tag{S-17}$$

If we assume that $S_{\alpha\alpha}(\omega)$ is slowly-varying in frequency for $|\omega - \omega_\mathrm{m}| \lesssim \gamma$ and that $\kappa_\mathrm{f} \gg \gamma$, this simplifies to

$$\Gamma_\phi|_{\Delta=\pm\omega_\mathrm{m}} = \eta n_\phi\left(\frac{\kappa_\mathrm{f}}{4}\left(1-\frac{2\kappa_\mathrm{e}}{\kappa}\right)^2 + \frac{\kappa_\mathrm{e}\gamma_\mathrm{OM}}{\kappa}\left(\frac{\gamma_\mathrm{OM}\kappa_\mathrm{e}}{\gamma\kappa} \pm \left(1-\frac{2\kappa_\mathrm{e}}{\kappa}\right)\right)\right). \tag{S-18}$$

Using the fact that $n_\phi = |\alpha|^2 S_{\phi\phi}(\omega_\mathrm{m}) \approx \omega_\mathrm{m}^2 n_\mathrm{c} S_{\phi\phi}(\omega_\mathrm{m})/\kappa_\mathrm{e}$, we obtain the contribution of phase noise to the noise-equivalent phonon number

$$n_{\mathrm{NEP},\phi}|_{\Delta=\pm\omega_\mathrm{m}} = \left(\frac{\omega_\mathrm{m}\kappa}{2\kappa_\mathrm{e} g_0}\right)^2 S_{\phi\phi}(\omega_\mathrm{m})\left(\frac{\kappa_\mathrm{f}}{4}\left(1-\frac{2\kappa_\mathrm{e}}{\kappa}\right)^2 + \frac{\kappa_\mathrm{e}\gamma_\mathrm{OM}}{\kappa}\left(\frac{\gamma_\mathrm{OM}\kappa_\mathrm{e}}{\gamma\kappa} \pm \left(1-\frac{2\kappa_\mathrm{e}}{\kappa}\right)\right)\right). \tag{S-19}$$

Like the pump-bleed through, phase noise leads to a constant contribution to n_NEP, and leads to squashing or anti-squashing of the noise depending on detuning and cooperativity, similar to heterodyne detection. Note, however, that in the case $\kappa_\mathrm{e}/\kappa = 0.5$ the contribution of phase noise will not depend upon detuning. Thus, even in the presence of large phase noise it is possible to avoid detuning dependent noise squashing/anti-squashing, though one will still have a large overall phase noise floor.

It is useful for characterization purposes to calculate the phase-noise contribution to the observed count rates when the laser is far-detuned from the cavity resonance ($|\Delta| \gg \omega_{\rm m}$). Assuming that the laser-filter detuning is kept constant at $\pm\omega_{\rm m}$, the phase-noise count rate in this case is just

$$\begin{aligned}\Gamma_\phi|_{|\Delta|\gg\omega_{\rm m}} &= \eta\int_{-\infty}^{\infty}\frac{d\omega}{2\pi}S_{\alpha\alpha}(\omega)|F(\omega,\pm\omega_{\rm m})|^2\\ &= \eta\frac{\kappa_{\rm f}}{4}n_\phi,\end{aligned} \tag{S-20}$$

with a corresponding noise-equivalent phonon number

$$n_{{\rm NEP},\phi}|_{|\Delta|\gg\omega_{\rm m}} = \left(\frac{\omega_{\rm m}\kappa}{4\kappa_{\rm e}g_0}\right)^2\kappa_{\rm f}S_{\phi\phi}(\omega_{\rm m}). \tag{S-21}$$

To get rid of the excess noise, we insert both the bandpass filter (for filtering spontaneous emission) and a tunable high-finesse filter (for filtering phase noise) immediately after the pump laser output as shown in Fig. S-1, enabling us to reach $n_{\rm NEP} \ll 1$ using a three-filter phonon counting setup as shown in Fig. 1d of the main text. A conservative estimate of the residual phase noise can be made by assuming that the limiting value of $n_{\rm NEP} \approx 4\times10^{-3}$ is entirely due to phase noise (i.e. perfect filtering of the pump tone). Using Eq. S-21 we find $S_{\phi\phi}(\omega_{\rm m}) \lesssim 8\times10^{-19}$ Hz^{-1}. For the pump power during the on-state of the pulse ($n_{\rm c,on} \approx 45$), the corresponding effective phase noise occupancy is $n_\phi \approx 3.2\times10^{-5}$, which has a negligible effect on the measurements in this work.

HEATING MODEL

The simplest thermal model assumes that the optically induced bath turns on instantaneously when the pulse is in the on-state. The corresponding rate equation for the phonon occupancy $\langle n\rangle$, for red- ($\Delta = \omega_{\rm m}$) and blue-detuned ($\Delta = -\omega_{\rm m}$) pulses during the on-state is thus

$$\dot{\langle n\rangle} = -\gamma\langle n\rangle + \gamma_{\rm p}n_{\rm p} + \gamma_0 n_0 + \frac{1}{2}\left(1\mp1\right)\gamma_{\rm OM}, \tag{S-22}$$

where $\gamma = \gamma_0 + \gamma_{\rm p} \pm \gamma_{\rm OM}$, $\gamma_{\rm p}$ and $n_{\rm p}$ are the coupling rate and occupancy of the hot phonon bath, γ_0 and n_0 are the coupling rate and occupancy of the ambient fridge bath, and the extra factor of $\gamma_{\rm OM}$ for a blue-detuned pump accounts for the possibility of spontaneous emission into the mechanical resonator due to the optomechanical interaction. This rate equation has the simple solution

$$\langle n\rangle(t) = \langle n\rangle(0)e^{-\gamma t} + n_{\rm H}\left(1-e^{-\gamma t}\right), \tag{S-23}$$

$$n_{\rm H} = \gamma^{-1}\left(\gamma_{\rm p}n_{\rm p} + \gamma_0 n_0 + \frac{1}{2}\left(1\mp1\right)\gamma_{\rm OM}\right). \tag{S-24}$$

where $\leq t \leq T_{\rm pulse}$.

In principle, $\gamma_{\rm OM}$ can be determined independently as described above, γ_0 can be determined by fitting the occupancy decay during the pulse off-state (Fig. 3 in the main text), while $\gamma_{\rm p}$ and $n_{\rm p}$ can be subsequently determined by fitting the steady-state occupancy curve shown in Fig. 1c of the main text. However, using these independently determined values in a fit to the red- and blue-detuned data shown in Fig. 2a of the main text results in a poor fit and inconsistent results. In particular, the apparent heating rate γ is much smaller than expected for a red-detuned pulse and larger than expected for a blue-detuned pulse. This, along with the "kink" in the heating curve shown in the inset of Fig. 2c of the main text, suggests additional complexity in the heating dynamics.

The simplest addition to the heating model is to assume a finite time for the hot phonon bath to come into equilibrium, which is approximated by allowing a fraction of the hot phonon bath occupancy to turn on exponentially over time. Thus, the phenomenological rate equation becomes

$$\dot{\langle n\rangle} = -\gamma\langle n\rangle + \gamma_{\rm p}n_{\rm p}\left(1-\delta_{\rm b}e^{-\gamma_{\rm S}t}\right) + \gamma_0 n_0 + \frac{1}{2}\left(1\mp1\right)\gamma_{\rm OM}, \tag{S-25}$$

where $\delta_{\rm b}$ is the slow growing fraction of $n_{\rm p}$ and $\gamma_{\rm S}$ the turn-on rate. Strictly speaking $\gamma_{\rm p}$ should depend on the phonon distribution of the hot phonon bath, and thus would be expected to be time-dependent in this model as well.

However, the resulting rate equation becomes intractable in such a case and the effects should be negligible in the regime $\gamma_{\rm OM} \gg \gamma_{\rm p}$, so we approximate $\gamma_{\rm p}$ equal to its steady-state value. This modified rate equation has the solution

$$\langle n\rangle(t) = \langle n\rangle(0)e^{-\gamma t} + n_{\rm H}\left(1-e^{-\gamma t}\right) + n_\delta\left(e^{-\gamma_{\rm S} t} - e^{-\gamma t}\right),\ n_\delta = \frac{\gamma_{\rm p} n_{\rm p}\delta_{\rm b}}{\gamma_{\rm S}-\gamma}, \tag{S-26}$$

which is used to obtain the fit shown in Fig. 2c of the main text with $\langle n\rangle(0)$, $\gamma_{\rm S}$ and $\delta_{\rm b}$ as free parameters.

During the off-state of the pulse ($T_{\rm pulse} \le t \le T_{\rm per}$), the resonator will simply cool towards the ambient fridge occupancy n_0 at the intrinsic damping rate γ_0. Using the initial condition that $\langle n\rangle(0) = n_0$ for the first pulse, and iterating many pulses we find that in the steady-state the initial phonon occupancy during a pulse (assuming $T_{\rm per} \gg T_{\rm pulse}$) is

$$\langle n\rangle(0) = \frac{n_0\left(1-e^{-\gamma_0 T_{\rm per}}\right) + n_{\rm H}\left(1-e^{-\gamma T_{\rm pulse}}\right)e^{-\gamma_0 T_{\rm per}} + n_\delta\left(e^{-\gamma_{\rm S} T_{\rm pulse}} - e^{-\gamma_{\rm S} T_{\rm per}}\right)e^{-\gamma_0 T_{\rm per}}}{1-e^{-\gamma T_{\rm pulse}-\gamma_0 T_{\rm per}}}. \tag{S-27}$$

Thus, once n_0, $\gamma_{\rm S}$ and $\delta_{\rm b}$ are determined by fitting the occupancy curves, we may use Eqs. S-26 and S-27 to determine the occupancy throughout the pulse for arbitrary $T_{\rm per}$ and $T_{\rm pulse}$. This allows us to determine the maximum attained phonon occupancy as a function of pulse parameters, as shown in Fig. 4a of the main text.

PHONON ADDITION/SUBTRACTION FIDELITY

In this section we present an analysis of heralded phonon addition and subtraction [6], including the effects of time-dependent, optically-induced heating to lowest order, with a particular eye towards the generation of single-phonon Fock states [7].

In a frame rotating at the pump frequency, the full Heisenberg-Langevin equations for the optomechanical system are [3]

$$\dot{\hat{a}} = -\left(i\Delta + \frac{\kappa}{2}\right)\hat{a} + ig_0\left(\hat{b}+\hat{b}^\dagger\right)\hat{a} + \sqrt{\kappa}\hat{a}_{\rm in}, \tag{S-28}$$

$$\dot{\hat{b}} = -\left(i\omega_{\rm m} + \frac{\gamma_{\rm b}}{2}\right)\hat{b} + ig_0\hat{a}^\dagger\hat{a} + \sqrt{\gamma_{\rm b}}\hat{b}_{\rm in}, \tag{S-29}$$

where $\hat{a}$, $\hat{b}$ are the photon and phonon annihilation operators, respectively, and $\hat{a}_{\rm in}$, $\hat{b}_{\rm in}$ are quantum noise operators corresponding to the optical and mechanical baths.

We linearize about a classical steady-state by displacing $\hat{a} \to \alpha + \hat{a}$, where $|\alpha|^2 = n_{\rm c}$. For concreteness we will consider the case $\Delta \equiv \omega_{\rm c} - \omega_{\rm l} = -\omega_{\rm m}$ (blue-detuned pump). Moving into a frame rotating at the mechanical frequency (i.e. $\hat{a} \to \hat{a}e^{i\omega_{\rm m}t}$, and so on for all operators), and making the rotating wave approximation, valid in the weak coupling ($g_0\sqrt{n_{\rm c}} \ll \kappa$) and sideband-resolved ($\kappa/\omega_{\rm m} \ll 1$) limit, we obtain

$$\dot{\hat{a}} = -\frac{\kappa}{2}\hat{a} + iG\hat{b}^\dagger + \sqrt{\kappa}\hat{a}_{\rm in}, \tag{S-30}$$

$$\dot{\hat{b}} = -\frac{\gamma_{\rm b}}{2}\hat{b} + iG\hat{a}_{\rm in}^\dagger + \sqrt{\gamma_{\rm b}}\hat{b}_{\rm in}, \tag{S-31}$$

where $G = g_0\sqrt{n_{\rm c}}$ and $\hat{a}_{\rm in}$, $\hat{b}_{\rm in}$ are the usual noise operators multiplied by $e^{-i\omega_{\rm m}t}$. The noise operators obey the following commutation and correlation relations

$$\left[\hat{a}_{\rm in}(t), \hat{a}_{\rm in}^\dagger(t')\right] = \left[\hat{b}_{\rm in}(t), \hat{b}_{\rm in}^\dagger(t')\right] = \delta(t-t') \tag{S-32}$$

$$\left\langle \hat{a}_{\rm in}(t)\hat{a}_{\rm in}^\dagger(t')\right\rangle = \delta(t-t') \tag{S-33}$$

$$\left\langle \hat{b}_{\rm in}^\dagger(t)\hat{b}_{\rm in}(t')\right\rangle = n_{\rm b}(t)\delta(t-t'), \quad \left\langle \hat{b}_{\rm in}(t)\hat{b}_{\rm in}^\dagger(t')\right\rangle = \left(n_{\rm b}(t)+1\right)\delta(t-t'). \tag{S-34}$$

Since we are working in the weak-coupling limit ($G \ll \kappa$) we may use the adiabatic solution for $\hat{a}$ (i.e. $\dot{\hat{a}} \approx 0$). Moreover, we wish to include the effects of mechanical noise to lowest order. Considering the effect of a short optical pulse of duration τ, we consider the case $\gamma_{\rm b}\tau, \gamma_{\rm b}\int_0^\tau ds\ n_{\rm b}(s) \ll 1$, as well as $\gamma_{\rm OM}\tau \ll 1$ and $\gamma_{\rm OM} \gg \gamma_{\rm b}$, where here $\gamma_{\rm OM} \equiv 4G^2/\kappa$ refers to the *magnitude* of the optomechanical damping rate (the sign will be explicitly incorporated for simplicity, since we're only considering blue-detuning). Under these assumptions, as in Ref. [8], the mechanical

noise term will be retained in the mechanical equation of motion only, since in the optical equations of motion it will acquire an extra factor of $\gamma_{\rm OM}\tau$ and thus can be neglected to lowest order. Furthermore, the $(\gamma_{\rm b}/2)\,\hat{b}$ term will be neglected in favor of the much larger $(\gamma_{\rm OM}/2)\,\hat{b}$ term. With these approximations, we arrive at the approximate equations

$$\hat{a} \approx i\sqrt{\frac{\gamma_{\rm OM}}{\kappa}}\hat{b}^\dagger + \frac{2}{\kappa}\hat{a}_{\rm in}, \tag{S-35}$$

$$\dot{\hat{b}} \approx \frac{\gamma_{\rm OM}}{2}\hat{b} + i\sqrt{\gamma_{\rm OM}}\hat{a}_{\rm in}^\dagger + \sqrt{\gamma_{\rm b}}\hat{b}_{\rm in}. \tag{S-36}$$

Formally integrating the equation of motion for $\hat{b}$ over the duration of the pulse while using the input-output relation for the optical cavity $\hat{a}_{\rm out} = -\hat{a}_{\rm in} + \sqrt{\kappa}\hat{a}$, we arrive at the approximate equations

$$\hat{a}_{\rm out}(t) = \hat{a}_{\rm in}(t) + i\sqrt{\gamma_{\rm OM}}e^{\frac{\gamma_{\rm OM}t}{2}}\hat{b}^\dagger(0) + \gamma_{\rm OM}e^{\frac{\gamma_{\rm OM}t}{2}}\int_0^t ds\; e^{\frac{-\gamma_{\rm OM}s}{2}}\hat{a}_{\rm in}(s) \tag{S-37}$$

$$\hat{b}(t) = e^{\frac{\gamma_{\rm OM}t}{2}}\hat{b}(0) + i\sqrt{\gamma_{\rm OM}}e^{\frac{\gamma_{\rm OM}t}{2}}\int_0^t ds\; e^{\frac{-\gamma_{\rm OM}s}{2}}\hat{a}_{\rm in}^\dagger(s) + \sqrt{\gamma_{\rm b}}e^{\frac{\gamma_{\rm OM}t}{2}}\int_0^t ds\; e^{\frac{-\gamma_{\rm OM}s}{2}}\hat{b}_{\rm in}(s). \tag{S-38}$$

We now introduce the following temporal modes [8]

$$\hat{B}_{\rm in} = \hat{b}(0), \quad \hat{B}_{\rm out} = \hat{b}(\tau), \tag{S-39}$$

$$\hat{A}_{\rm in} = \sqrt{\frac{\gamma_{\rm OM}}{1-e^{-\gamma_{\rm OM}\tau}}}\int_0^\tau ds\; e^{\frac{-\gamma_{\rm OM}s}{2}}\hat{a}_{\rm in}(s), \tag{S-40}$$

$$\hat{A}_{\rm out} = \sqrt{\frac{\gamma_{\rm OM}}{e^{\gamma_{\rm OM}\tau}-1}}\int_0^\tau ds\; e^{\frac{\gamma_{\rm OM}s}{2}}\hat{a}_{\rm out}(s) \tag{S-41}$$

$$\hat{F} = \sqrt{\gamma_{\rm b}}e^{\frac{\gamma_{\rm OM}\tau}{2}}\int_0^\tau ds\; e^{\frac{-\gamma_{\rm OM}s}{2}}\hat{b}_{\rm in}(s), \tag{S-42}$$

which allows us to rewrite the input/output equations at the end of the pulse ($t=\tau$)

$$\hat{A}_{\rm out} = e^{\frac{\gamma_{\rm OM}\tau}{2}}\hat{A}_{\rm in} + i\sqrt{e^{\gamma_{\rm OM}\tau}-1}\hat{B}_{\rm in}^\dagger, \tag{S-43}$$

$$\hat{B}_{\rm out} = e^{\frac{\gamma_{\rm OM}\tau}{2}}\hat{B}_{\rm in} + i\sqrt{e^{\gamma_{\rm OM}\tau}-1}\hat{A}_{\rm in}^\dagger + \hat{F}. \tag{S-44}$$

Note that $[\hat{A}_{\rm in},\hat{A}_{\rm in}^\dagger] = [\hat{A}_{\rm out},\hat{A}_{\rm out}^\dagger] = [\hat{B}_{\rm in},\hat{B}_{\rm in}^\dagger] = 1$ as expected. As for the noise operator $\hat{F}$, the commutator and correlation functions are defined, using the known properties of $\hat{b}_{\rm in}(t)$ to lowest order as

$$[\hat{F},\hat{F}^\dagger] \approx \gamma_{\rm b}\tau + O(\gamma_{\rm OM}\gamma_{\rm b}\tau^2), \tag{S-45}$$

$$\left\langle \hat{F}^\dagger\hat{F}\right\rangle = \gamma_{\rm b}e^{\gamma_{\rm OM}\tau}\int_0^\tau ds\; e^{-\gamma_{\rm OM}s}n_{\rm b}(s), \quad \left\langle \hat{F}\hat{F}^\dagger\right\rangle = \gamma_{\rm b}\tau + \left\langle \hat{F}^\dagger\hat{F}\right\rangle. \tag{S-46}$$

We now seek a unitary propagator $\hat{U}$ such that $\hat{A}_{\rm out} = \hat{U}^\dagger\hat{A}_{\rm in}\hat{U}$ and $\hat{B}_{\rm out} = \hat{U}^\dagger\hat{B}_{\rm in}\hat{U}$. Note that if we define $e^{\gamma_{\rm OM}\tau/2} = \cosh(r), \sqrt{e^{\gamma_{\rm OM}\tau}-1} = \sinh(r)$, then the input/output equations have the form of two-mode squeezing between $\hat{A}_{\rm in}$ and $\hat{B}_{\rm in}$ in the absence of mechanical noise $\hat{F}$. Thus, we want $\hat{U} = \hat{U}_{\rm m}\hat{U}_0$ where

$$\hat{U}_0 = e^{ir\left(\hat{A}_{\rm in}\hat{B}_{\rm in} + \hat{A}_{\rm in}^\dagger\hat{B}_{\rm in}^\dagger\right)}, \tag{S-47}$$

$$\hat{U}_{\rm m}^\dagger\hat{B}_{\rm in}\hat{U}_{\rm m} = \hat{B}_{\rm in} + \hat{F}, \tag{S-48}$$

$$[\hat{U}_{\rm m},\hat{A}_{\rm in}] = 0. \tag{S-49}$$

We find that a beam-splitter type interaction between $\hat{B}_{\rm in}$ and $\hat{F}$ satisfies this condition to lowest order. That is, if $\hat{U}_{\rm m} = e^{\hat{B}_{\rm in}^\dagger\hat{F} - \hat{B}_{\rm in}\hat{F}^\dagger}$, then using the above commutation relations for $\hat{F}$ we can show,

$$\begin{aligned}\hat{U}_{\rm m}^\dagger\hat{B}_{\rm in}\hat{U}_{\rm m} &= \cos\left(\sqrt{\gamma_{\rm b}\tau}\right)\hat{B}_{\rm in} + \left(\gamma_{\rm b}\tau\right)^{-1/2}\sin\left(\sqrt{\gamma_{\rm b}\tau}\right)\hat{F} \\ &\approx \hat{B}_{\rm in} + \hat{F}.\end{aligned} \tag{S-50}$$

Given this propagator $\hat{U}$ which yields the approximate system evolution over the pulse interval τ, and assuming an initial density matrix $\rho_0 = |0_\mathrm{A}\rangle\langle 0_\mathrm{A}| \otimes \rho_{\mathrm{B},0} \otimes \rho_\mathrm{F}$, where A, B, and F refer to the optical, mechanical, and bath subsystems respectively, the density matrix for the mechanical resonator, ρ_B, conditioned upon detection of a single photon, is given by

$$\begin{aligned}\rho_\mathrm{B} &= \frac{\mathrm{Tr}_{\mathrm{A,F}}\left(|1_\mathrm{A}\rangle\langle 1_\mathrm{A}| \otimes I_\mathrm{B} \otimes I_\mathrm{F}\hat{U}\rho_0\hat{U}^\dagger\right)}{\mathrm{Tr}\left(|1_\mathrm{A}\rangle\langle 1_\mathrm{A}| \otimes I_\mathrm{B} \otimes I_\mathrm{F}\rho_0\right)} \\ &= P^{-1}\mathrm{Tr}_\mathrm{F}\left(\hat{U}_\mathrm{m}\langle 1_\mathrm{A}|\hat{U}_0\rho_0\hat{U}_0^\dagger|1_\mathrm{A}\rangle\hat{U}_\mathrm{m}^\dagger\right),\end{aligned} \tag{S-51}$$

where P is the overall probability of photodetection, given by

$$P = \mathrm{Tr}_\mathrm{B}\left(\langle 1_\mathrm{A}|\hat{U}_0|0_\mathrm{A}\rangle\langle 0_\mathrm{A}| \otimes \rho_{\mathrm{B},0}\hat{U}_0^\dagger|1_\mathrm{A}\rangle\right). \tag{S-52}$$

Denoting $\rho_{\mathrm{B,ideal}} = P^{-1}\hat{B}_\mathrm{in}^\dagger\rho_{\mathrm{B},0}\hat{B}_\mathrm{in}$ as the ideal conditional matrix in the absence of mechanical dissipation, and expanding $\hat{U}$ to lowest order in $\gamma_\mathrm{OM}\tau$, $\gamma_\mathrm{b}\tau$ and $\left\langle\hat{F}^\dagger\hat{F}\right\rangle$, we find

$$P \approx \gamma_\mathrm{OM}\tau\left\langle\hat{B}_\mathrm{in}^\dagger\hat{B}_\mathrm{in}\right\rangle, \tag{S-53}$$

and

$$\begin{aligned}\rho_\mathrm{B} \approx &\left(1-\left\langle\hat{F}^\dagger\hat{F}\right\rangle\right)\rho_\mathrm{B,ideal} + \left\langle\hat{F}^\dagger\hat{F}\right\rangle\hat{B}_\mathrm{in}^\dagger\rho_\mathrm{B,ideal}\hat{B}_\mathrm{in} + \left(\gamma_\mathrm{b}\tau + \left\langle\hat{F}^\dagger\hat{F}\right\rangle\right)\hat{B}_\mathrm{in}\rho_\mathrm{B,ideal}\hat{B}_\mathrm{in}^\dagger \\ &- \frac{1}{2}\left(\gamma_\mathrm{b}\tau + 2\left\langle\hat{F}^\dagger\hat{F}\right\rangle\right)\left(\hat{B}_\mathrm{in}^\dagger\hat{B}_\mathrm{in}\rho_\mathrm{B,ideal} + \rho_\mathrm{B,ideal}\hat{B}_\mathrm{in}^\dagger\hat{B}_\mathrm{in}\right).\end{aligned} \tag{S-54}$$

To evaluate the fidelity of the phonon addition subtraction, we use the definition of fidelity between two quantum states ρ_1 and ρ_2, given by [9] $F = \mathrm{Tr}\left(\sqrt{\rho_1^{1/2}\rho_2\rho_1^{1/2}}\right)$, which is straightforward to evaluate for an initial thermal mechanical state, as both ρ_1 and ρ_2 will be diagonal in the Fock state basis.

Note that the only substantive difference in the case of phonon subtraction ($\Delta = \omega_\mathrm{m}$, red-detuned pumping) is that the propagator $\hat{U}_0$ will have the form of a beam-splitter interaction rather than two mode squeezing. This will only change P and $\rho_\mathrm{B,ideal}$, which are now given by

$$P \approx \gamma_\mathrm{OM}\tau\left\langle\hat{B}_\mathrm{in}^\dagger\hat{B}_\mathrm{in}\right\rangle, \tag{S-55}$$

$$\rho_\mathrm{B,ideal} = \hat{B}_\mathrm{in}\rho_{\mathrm{B},0}\hat{B}_\mathrm{in}^\dagger, \tag{S-56}$$

while the definition of ρ_B in terms of $\rho_\mathrm{B,ideal}$ is unchanged assuming that the bath heating is only dependent on pump power and not pump detuning. To evaluate the fidelity of the creation of a single phonon Fock state [7] in our system as a function of pulse width and period for blue-detuned pulses, we assume the initial state of the mechanics to be a thermal state with average phonon number $\langle n\rangle$ given by Eq. S-27, while $\left\langle\hat{F}^\dagger\hat{F}\right\rangle$ can be evaluated using the fit parameters of the effective time-dependent hot phonon bath. We may then calculate the conditional density matrix via Eq. S-54 and the fidelity by setting $\rho_1 = |1_\mathrm{B}\rangle\langle 1_\mathrm{B}|$ and $\rho_2 = \rho_\mathrm{B}$.

* Electronic address: opainter@caltech.edu

[1] J. D. Cohen, S. M. Meenehan, G. S. MacCabe, S. Gröblacher, A. H. Safavi-Naeini, F. Marsili, M. D. Shaw, and O. Painter, arXiv:1410.1047 (2014).
[2] F. Marsili, V. B. Verma, J. A. Stern, S. Harrington, A. E. Lita, T. Gerrits, I. Vayshenker, B. Baek, M. D. Shaw, R. P. Mirin, et al., Nature Photon. **7**, 210 (2013).
[3] A. H. Safavi-Naeini, J. Chan, J. T. Hill, S. Gröblacher, H. Miao, Y. Chen, M. Aspelmeyer, and O. Painter, New J. Phys. **15**, 035007 (2013).
[4] M. Poggio, C. L. Degen, H. J. Mamin, and D. Rugar, Phys. Rev. Lett. **99**, 017201 (2007).
[5] T. Rocheleau, T. Ndukum, C. Macklin, J. B. Hertzberg, A. A. Clerk, and K. C. Schwab, Nature **463**, 72 (2010).
[6] M. R. Vanner, M. Aspelmeyer, and M. S. Kim, Phys. Rev. Lett. **110**, 010504 (2013).
[7] C. Galland, N. Sangouard, N. Piro, N. Gisin, and T. J. Kippenberg, Phys. Rev. Lett. **112**, 143602 (2014).
[8] S. G. Hofer, W. Wieczorek, M. Aspelmeyer, and K. Hammerer, Phys. Rev. A **84**, 052327 (2011).
[9] M. Nielsen and I. Chuang, *Quantum Computation and Quantum Information* (Cambridge University Press, 2000).